Title

Two Endosomal NHX-type Na^+/ H^+ Antiporters are Involved in Auxin Mediated Development in *Arabidopsis thaliana*

Running head

Arabidopsis NHXs in auxin mediated development

Corresponding author

A. R. Gendall

Department of Animal, Plant and Soil Sciences, AgriBio, Centre for AgriBiosciences, 5 Ring Road, La Trobe University, Bundoora, VIC 3086, Australia

Telephone: +61 3 9032 7466

Email: T.Gendall@latrobe.edu.au

Subject areas

Growth and development, Membrane and transport

Number of black and white figures, color figure, tables and type and number of supplementary materials

Black and white figures: 1

Colour figures: 5

Supplementary Figures: 5

Supplementary Tables: 1

Title

Two Endosomal NHX-type Na^+/ H^+ Antiporters are Involved in Auxin Mediated Development in *Arabidopsis thaliana*

Running head

Arabidopsis NHXs in auxin mediated development

Authors

Jonathan Michael Dragwidge[1], Brett Andrew Ford[1,2], Joanne Rachel Ashnest[1,3], Partha Das[1,4] and Anthony Richard Gendall[1]*

[1]Department of Animal, Plant and Soil Sciences, AgriBio, Centre for AgriBiosciences, 5 Ring Road, La Trobe University, Bundoora, VIC 3086, Australia

Present Addresses:

[2] Agriculture and Food, Commonwealth Scientific and Industrial Research Organisation, Clunies Ross Street, Acton, ACT 2601, Australia

[3] Global Institute for Food Security, 110 Gymnasium Place, University of Saskatchewan, Saskatoon, S7N4J8, Canada

[4] College of Agriculture, Tripura, Lembucherra, 799210, India

*email: T.Gendall@latrobe.edu.au

Abbreviations:

1-NAA, 1-naphthaleneacetic acid; BFA, brefeldin A; CHX, cycloheximide; EE, early endosome; GFP, green fluorescent protein; GUS, β-glucuronidase; LRP, lateral root primordia; LR, lateral root; MVB, multi-vesicular body; NHX, sodium-hydrogen exchanger; PIN, pin-formed; PVC, pre-vacuolar compartment; TGN, *trans*-Golgi network;

Abstract

In *Arabidopsis thaliana*, the endosomal localised Na^+/H^+ antiporters NHX5 and NHX6 regulate ion and pH homeostasis and are important for plant growth and development. However, the mechanism of how these endosomal NHXs function in plant development is not well understood. Auxin modulates plant growth and development through the formation of concentration gradients in plant tissue to control cell division and expansion. Here, we identified a role for NHX5 and NHX6 in the establishment and maintenance of auxin gradients in embryo and root tissues. We observed developmental impairment and abnormal cell division in embryo and root tissues in the double knockout *nhx5 nhx6*, consistent with these tissues showing high expression of *NHX5* and *NHX6*. Through confocal microscopy imaging with the *DR5::GFP* auxin reporter, we identify defects to the perception, accumulation, and redistribution of auxin in *nhx5 nhx6* cells. Furthermore, we find that the steady state levels of the PIN-FORMED (PIN) auxin efflux carriers PIN1 and PIN2 are reduced in *nhx5 nhx6* root cells. Our results demonstrate that NHX5 and NHX6 function in auxin mediated plant development by maintaining PIN abundance at the plasma membrane, and provides new insight into the regulation of plant development by endosomal NHX antiporters.

Key Words: auxin, lateral root, NHX5, NHX6, PIN, *Arabidopsis thaliana*

Introduction

The ability to regulate cellular ion and pH homeostasis is a basic requirement of all living organisms, particularly under abiotic stress. In part this is achieved through a family of specialised Na^+/H^+ exchangers (NHXs) which utilise an electrochemical gradient to transport a Na^+ or K^+ ion for H^+ across a membrane (Blumwald, 2000). NHXs are found in all eukaryotes, and apart from their roles in pH and ion homeostasis, also function in diverse processes including the regulation of cell shape and volume, vesicular trafficking, protein sorting, and cellular stress responses (Bassil et al., 2012; Brett et al., 2005a; Chanroj et al., 2012; Ohgaki et al., 2011; Orlowski and Grinstein, 2007). In *Arabidopsis thaliana* two intracellular NHXs, NHX5 and NHX6, act redundantly, and have a significant role in plant growth and development (Bassil et al., 2011). Double knockout *nhx5 nhx6* plants display growth abnormalities, including a dwarf phenotype, and reduced shoot and root growth due to slowed cell proliferation (Bassil et al., 2011). All sequenced plant species examined to date have NHX5 and NHX6 orthologs, demonstrating the importance of endosomal NHXs for plant function (Chanroj et al., 2012; Ford et al., 2012).

Recent evidence has implicated plant NHXs in subcellular protein trafficking. In *Arabidopsis thaliana,* NHX5 and NHX6 localise to the Golgi, *trans*-Golgi network/early endosome (TGN/EE), and the multi-vesicular body/pre-vacuolar compartment (MVB/PVC) where they regulate lumenal pH homeostasis (Bassil et al., 2011; Reguera et al., 2015). *nhx5 nhx6* mutants fail to correctly sort a vacuolar-targeted yeast carboxypeptidase Y (CPY) GFP fusion protein, and have delayed trafficking of the endocytic tracer dye FM4-64 to the vacuole, demonstrating a clear role of NHX5 and NHX6 in vacuolar trafficking (Bassil et al., 2011). Furthermore, NHX5 and NHX6 are required for normal processing and transport of seed storage proteins to the protein storage vacuole in embryos (Ashnest et al., 2015; Reguera et al., 2015). Similar vacuolar trafficking defects have been observed in the yeast *nhx1* mutant (Bowers et al., 2000; Brett et al., 2005b), and in animal cells where the mammalian orthologs *NHE6* and *NHE8* genes have been silenced by RNAi (Lawrence et al., 2010; Ohgaki et al., 2010), demonstrating that this class of NHX proteins has a conserved role in sub-cellular trafficking across multiple phyla.

The strong reported expression of *NHX6* in developing embryos (Ashnest et al., 2015), along with inhibited root and shoot growth in *nhx5 nhx6* (Bassil et al., 2011) implicate a role for NHX5 and NHX6 in both embryonic and post-embryonic plant development. The phytohormone auxin is vital for normal

plant development, and regulates essential processes including cell patterning, meristem identity and tropisms (Petrásek and Friml, 2009). The asymmetric distribution of auxin in cells is generated through polar auxin transport, which drives the generation of defined auxin gradients and maxima in plant tissues. Auxin gradients are formed and maintained through directional inter-cellular auxin transport mediated by the auxin influx AUX1/LIKE-AUX1 (AUX1/LAX) and auxin efflux PIN FORMED (PIN) families of carrier proteins (Friml, 2010; Marchant et al., 2002; Wisniewska et al., 2006). Auxin gradients generated through PIN and AUX carriers are essential for controlling cell division and differentiation in the root tip and developing lateral root primordia, as well as during embryogenesis and shoot organogenesis (Möller and Weijers, 2009; Petrásek and Friml, 2009).

Maintenance of AUX and PIN polarity at the plasma membrane is essential for directional intercellular auxin transport, and relies on the dynamic trafficking of these carriers through multiple subcellular pathways. PINs undergo constitutive endocytosis from the plasma membrane to the TGN/EE (Dhonukshe et al., 2007; Geldner et al., 2001), which acts as the hub of endocytic and secretory traffic in plant cells (Viotti et al., 2010). The polar recycling of PINs to the basal plasma membrane from the TGN/EE is mediated by a pathway involving the Brefeldin A (BFA) sensitive ARF guanine-nucleotide exchange factor (ARF-GEF) GNOM (Geldner et al., 2003). Conversely, apical trafficking of PIN2 and AUX1 occurs through a GNOM-independent pathway distinct from that of basal trafficking of PIN1 (Kleine-Vehn et al., 2006; Robert et al., 2008), highlighting that distinct basal and apical transport routes exist.

PIN carriers also undergo vacuolar degradation which assists in controlling their abundance at the plasma membrane. Internalised PIN proteins targeted for degradation are trafficked to the MVB/PVC for sorting into endosomal intraluminal vesicles, before final delivery to the lytic vacuole for degradation (Kleine-Vehn et al., 2008; Spitzer et al., 2009). This vacuolar degradation pathway is regulated by the retromer complex, which is thought to enable the retrieval of PIN proteins from the MVB/PVC, thus maintaining PIN polarity and abundance at the plasma membrane (Jaillais et al., 2006; Kleine-Vehn et al., 2008; Nodzynski et al., 2013). We recently reported that the C-terminal cytosolic tail of NHX6 interacts with the retromer complex component SORTING NEXIN1 (SNX1), and NHX5 and SNX1 strongly co-localise in endosomal compartments in root cells, suggesting that NHX5 and NHX6 may be involved in retromer-mediated PIN recycling (Ashnest et al., 2015).

Although phenotypic evidence supports a role for NHX5 and NHX6 in embryo and root development, the underlying mechanism behind their contribution has not been investigated. Here, through promoter-reporter assays we show that *NHX6* is expressed in the primary root and developing lateral roots. Furthermore, we identify defects in embryo and lateral root primordia development in *nhx5 nhx6* mutants, and link these defects to a disruption in auxin signalling due to reduced PIN1 and PIN2 protein abundance at the plasma membrane. Finally, pharmacological interference of PIN1 and PIN2 recycling indicate that NHX5 and NHX6 function independently of polar PIN recycling pathways, and instead may be implicated in retromer controlled PIN degradation. These findings demonstrate that NHX5 and NHX6 are important for functional auxin mediated plant development.

Results

NHX6 is expressed in primary and developing lateral roots

NHX5 and *NHX6* have been reported to be expressed in whole root tissue (Bassil et al., 2011; Yokoi et al., 2002). To more closely examine the expression of *NHX6* in roots, we created a β-glucuronidase (GUS) reporter construct driven by 3 kb of sequence upstream of the start codon of *NHX6* (Ashnest et al., 2015). In the primary root, GUS activity was strongly observed in the apical meristematic zone, stem cell niche and columella cells in multiple independent lines (Figure 1A). This strong *NHX6* expression in root tip columella cells is consistent with findings from microarray expression profiles (Brady et al., 2007). GUS activity was also detected in the central primordia cells of early stage (II to V) developing lateral root primordia (LRP), ubiquitously in late stage (VII) primordia, and confined to the vascular tissue in emerging and mature lateral roots (Figure 1A). A similar construct containing up to 3 kb of the *NHX5* promoter failed to produce any GUS staining, suggesting additional elements may be required for *NHX5* expression in the root.

nhx5 nhx6 mutants exhibit disturbed lateral root development

The double knockout *nhx5-1 nhx6-1* was originally characterised with a dwarf plant phenotype and reduced primary root growth (Bassil et al., 2011). To identify the cause of this defect, we examined *nhx5 nhx6* roots in detail using a second allelic combination which we reported show identical seed storage protein phenotypes to *nhx5-1 nhx6-1* (*nhx5-2 nhx6-3*; see Material and Methods, Ashnest et al., 2015). Consistent with previous reports, primary root length of *nhx5-2 nhx6-3* seedlings was significantly

reduced, with a large proportion of seedlings exhibiting arrested development shortly after cotyledon expansion (Figure 1C and S1A; Bassil et al., 2011). These phenotypes could be completely rescued by growing *nhx5 nhx6* seedlings on media supplemented with sucrose (Figure S1), a phenotype shared by mutants with defects in vacuolar trafficking (Feraru et al., 2010; Kleine-Vehn et al., 2008; Shimada et al., 2006).

We next determined if LRP development was affected in *nhx5 nhx6* mutants. Lateral roots develop through a series of highly coordinated cell divisions before eventually emerging from the primary root (Malamy and Benfey, 1997; Vilches-Barro and Maizel, 2015). We observed and quantified LRP development from initiation through to emergence by crossing the plasma membrane localised *pAUX1-AUX1-YFP* marker into *nhx5 nhx6*. No gross morphological defects were present in LRP from *nhx5 nhx6* seedlings, indicating that their cellular patterning and organisation is not dramatically affected (Figure 1B). LRP density was increased in *nhx5 nhx6* plants (Figure 1D), consistent with a reduction in root length due to slowed cell expansion (Bassil et al., 2011), but normal LRP initiation. However, we occasionally observed the formation of ectopic LRP (Figure S2), suggesting that the distribution of LRP initiation events along the primary root may be disrupted. Moreover, *nhx5 nhx6* mutants showed an increase of early stage LRP, but decrease in late stage LRP (Figure 1E), indicating a delay to, or inhibition of LRP development. An estradiol-inducible NHX6-GFP rescue construct could partially restore both primary root elongation and lateral root emergence in *nhx5 nhx6* seedlings germinated and grown in the presence of the inducer, confirming that knock-out of endosomal NHXs are responsible for these phenotypes (Figure S4).

Embryo patterning is altered in nhx5 nhx6

We previously reported *NHX6* promoter-GUS activity in developing and mature stage embryos (Ashnest et al., 2015), indicating that NHX6 is expressed during embryo development. We thus investigated whether *nhx5 nhx6* mutants may display abnormalities during embryogenesis. Morphological assessment of cleared embryos revealed low penetrance cell patterning defects throughout globular, triangle, and heart stages of development in *nhx5 nhx6* (Figure 2). Defects were apparent in the basal cell region corresponding to the embryonic root, along with cell patterning anomalies in the tips of the incipient cotyledons. Together with primary and lateral root data, these findings indicate that NHX5 and NHX6 function in both embryo and root growth and development, two tissues that are critically

associated with auxin patterning.

Auxin gradients and maxima are disrupted in nhx5 nhx6

The phytohormone auxin is critical for meristem growth and cellular patterning in the root tip, and for the initiation, development and emergence of lateral roots (Petrásek and Friml, 2009). We questioned whether the disruption to lateral root primordia initiation and development in *nhx5 nhx6* is a result of auxin related defects. To investigate this, we assessed auxin response maxima in *nhx5 nhx6* mutant plants homozygous for the auxin-activity reporter *pDR5rev::GFP* (Benková et al., 2003). Visualisation of *DR5::GFP* expression in the primary root tip of *nhx5 nhx6* seedlings revealed strong expression in the quiescent centre and columella root cap cells, similar to the expression in wild type (Figure 3A), indicating no obvious defect to auxin maxima at the root tip. The *DR5* auxin response marker is also clearly expressed in the tip of LRP from Stage IV/V onwards (Dubrovsky et al., 2008). Interestingly, *DR5* expression in late stage LRP of *nhx5 nhx6* mutants was diffuse, with less clearly defined auxin maxima at the primordia tip (Figure 3B), indicating that auxin response is disrupted in these cells.

Auxin plays a major role in embryogenesis and leaf development, with auxin gradients controlling the formation of the apical-basal axis and co-ordinating cell division in the embryo and leaf (Möller and Weijers, 2009; Scarpella et al., 2006). Given the disruption to cellular patterning in *nhx5 nhx6* embryos, we assessed if similar defects in auxin response were present as in the LRP. In wild type embryos from the triangle stage onwards, *DR5* auxin response maxima are present in the basal cells and in the tips of the incipient cotyledons (Figure 3C) (Benková et al., 2003). In triangle and heart stage *nhx5 nhx6* embryos, *DR5::GFP* auxin reporter maxima were visibly reduced in the basal region, and undetectable in the apical embryo tips, demonstrating a disruption to auxin maxima in these cells. Furthermore, we also occasionally observed defects in leaf patterning in young *nhx5 nhx6* seedlings which were accompanied by a reduction in *DR5* expression. This finding is consistent with recent evidence reporting reduced *DR5::GUS* staining in *nhx5 nhx6* rosettes (Fan et al., 2018). Taken together, these results show that NHX5 and NHX6 play a role in auxin-mediated plant development in multiple tissues.

nhx5 nhx6 mutants exhibit auxin insensitivity and reduced gravitropic response

The dwarf phenotype and inhibited root growth of *nhx5 nhx6* mutants (Bassil et al., 2011), as well as the auxin-dependent defects reported here suggest that their perception and/or response to auxin may

be disrupted. To investigate this, we tested the response of *nhx5 nhx6* seedlings to the synthetic auxin analogue 1-naphthaleneacetic acid (1-NAA). Exogenous auxin treatment inhibits root elongation and causes rapid proliferation of lateral root primordia. Root growth assays revealed *nhx5 nhx6* seedlings were less sensitive than wild type to inhibition of root elongation by 1-NAA at concentrations of 250 nM and higher (Figure 4A), typical of mutants insensitive to auxin (Ambrose et al., 2013; Booker et al., 2003). Next, we assessed if *nhx5 nhx6* were insensitive to the induction of lateral root initiation by 1-NAA treatment. Although LRP were initiated in *nhx5 nhx6* roots in response to 1-NAA, they were underdeveloped with abnormal spacing, and often exhibited weak *DR5* expression (Figure 4B), and emerged at lower frequency than in wildtype plants (Figure 4C). These abnormalities are consistent with the defects in auxin maxima in *nhx5 nhx6* lateral root primordia, and suggest that *nhx5 nhx6* mutants have reduced auxin transport capability necessary to generate functional auxin gradients in the root.

Root gravitropism requires the coordinated asymmetrical distribution of auxin in the root meristem (Petrásek and Friml, 2009). As we identified a possible disruption to auxin transport in *nhx5 nhx6* roots, we tested whether root gravitropic response was affected. In response to gravity stimulus, *nhx5 nhx6* seedlings showed slower root re-orientation compared to wild type seedlings (Figure 4D). Furthermore, we assessed whether auxin response and redistribution in *nhx5 nhx6* may be altered in response to gravity. *nhx5 nhx6* seedlings also showed a reduction in the redistribution of auxin to the lower root side after gravistimulation (Figure 4E). Thus, the reduced gravitropic response in *nhx5 nhx6* is likely due to a reduced ability to redistribute auxin in the root meristem. The coordinated asymmetrical distribution of auxin in root gravitropic response is dependent on PIN2 activity (Abas et al., 2006; Kleine-Vehn et al., 2008), indicating that normal PIN2 function could be disrupted in *nhx5 nhx6*. Taken together, these data support our findings suggesting *nhx5 nhx6* mutants have a reduced ability to perceive and transport auxin in the root.

PIN1 and PIN2 abundance is reduced in nhx5 nhx6 roots

To determine if the disruption to auxin gradients and maxima in *nhx5 nhx6* tissues is the result of a disturbance in auxin carrier protein abundance or polarity, we first investigated the localisation of the AUX/LAX carrier pAUX1:AUX1-YFP in the primary root meristem of *nhx5 nhx6*. AUX1 localises to epidermal cells in the root meristem, as well as on the apical plasma membrane in the protophloem

(Kleine-Vehn et al., 2006; Swarup et al., 2001). AUX1-YFP polarity and abundance in protophloem and epidermal cells was unaffected in *nhx5 nhx6* (Figure 5A and S3), suggesting that the auxin related defects may occur independently of AUX1 activity.

We next enquired whether the reduced gravitropic response and impaired ability to redistribute auxin in *nhx5 nhx6* might be associated with changes in PIN distribution or abundance. In the primary root meristem, PIN1 localises to the basal plasma membrane of stele cells to direct auxin towards the tip, while PIN2 localises to the apical plasma membrane of epidermal and cortex cells to direct auxin towards the elongation zone (Blilou et al., 2005; Abas et al., 2006; Wisniewska et al., 2006). The expression domain and polarity of pPIN1:PIN1-GFP and pPIN2:PIN2-GFP remained unaffected in *nhx5 nhx6* root tips (Figure 5B and 5C), indicating that trafficking of PIN1 and PIN2 to the basal or apical plasma membrane respectively occurs normally. However, fluorescence intensity levels of PIN1-GFP and PIN2-GFP at the plasma membrane were markedly lower in *nhx5 nhx6* compared to wild type (Figure 5B-D), demonstrating that the steady state level of these proteins is disrupted. Furthermore, the signal intensity of PIN1-GFP was also reduced in the provascular cells of stage IV-VII LRP in *nhx5 nhx6* roots (Figure 5E), consistent with the inhibited *DR5* gradients in these cells. These findings suggest that the reduced PIN abundance in root tissue may be related to the disruption of auxin gradients and maxima in *nhx5 nhx6.*

NHX5 and NHX6 are not involved in polar PIN trafficking

To test if NHX5 and NHX6 are directly involved in trafficking of PIN1 or PIN2 to the plasma membrane, we examined the response of PIN1 and PIN2 to BFA inhibition. BFA interferes with ARF-guanine-exchange factor (GEF) GNOM function, and results in the internalisation of PIN1 and PIN2 protein into a core BFA compartment composed of aggregated TGN/EE vesicles (Geldner et al., 2003, 2001; Naramoto et al., 2014). We pre-treated root epidermal cells expressing PIN1-GFP and PIN2-GFP with cycloheximide (CHX) to inhibit protein synthesis, followed by CHX+BFA treatment, in order to examine PIN1 and PIN2 cycling between the TGN/EE and the plasma membrane. Response to BFA treatment and washout of PIN1-GFP and PIN2-GFP in *nhx5 nhx6* was similar to wild type seedlings (Figure 6), suggesting that NHX5 and NHX6 are not directly involved in the polar transport of either PIN1 or PIN2. This finding indicates that while NHX5 and NHX6 are important for the maintenance of PIN1 and PIN2 steady state levels at the plasma membrane, they are not required for the establishment or maintenance

of PIN1 or PIN2 polarity.

Discussion

In this study, we identified a role for NHX5 and NHX6 in auxin mediated embryonic and post-embryonic growth and development. Detailed characterisation of the double knockout *nhx5 nhx6* revealed cell patterning and growth defects during embryogenesis and lateral root primordia development. Through confocal microscopy imaging we identified a disruption in *DR5* auxin perception, accumulation and redistribution in *nhx5 nhx6* seedlings. Furthermore, in *nhx5 nhx6* root cells we found that PIN1-GFP and PIN2-GFP abundance was altered, but not their polar trafficking to the plasma membrane.

NHX5 and NHX6 are important for root and embryo development

In addition to previously reported expression of *pNHX6:GUS* in the developing embryo (Ashnest et al., 2015), strong promoter activity was observed in the primary root meristem and throughout lateral root primordia development. These findings correlate with previous microarray and semi-quantitative RT-PCR experiments demonstrating that *NHX5* and *NHX6* are expressed in all root tissues (Bassil et al., 2011; Brady et al., 2007; Yokoi et al., 2002). Furthermore, the highly spatial and temporal expression in the early to mid LRP suggests a specific role for NHX6 in lateral root development. This finding is consistent with the disturbed development and emergence of lateral root primordia, and cellular patterning defects in radicle cells in developing embryos in*nhx5 nhx6* double knockouts.

NHX5 and NHX6 play roles in auxin mediated plant development through maintaining PIN homeostasis

We found that developmental patterning defects in the embryo and lateral root primordia in *nhx5 nhx6* were correlated with a reduction in *DR5-GFP* expression, indicating a disruption to the establishment of auxin gradients in these tissues. Furthermore, gravitropism and synthetic auxin (1-NAA) experiments revealed auxin perception and redistribution in the *nhx5 nhx6* root is impaired. The generation of functional auxin gradients is required for correct cellular division and patterning during embryogenesis, root meristem growth, and lateral root primordia formation and development (Benková et al., 2003; Blilou et al., 2005; Möller and Weijers, 2009; Robert et al., 2015). Our results demonstrate that the defects to cellular patterning and growth in *nhx5 nhx6* are largely auxin dependent. Thus, loss of NHX5 and NHX6 appears to interfere with the generation and establishment of auxin gradients during plant tissue development, with auxin pereception and signalling aslo likely to be affected. Interestingly, it has

been reported that free indole-3-acetic acid (IAA) and IAA-conjugate metabolites are altered in *nhx5 nhx6* Arabidopsis roots, suggesting NHX5 and NHX6 may also affect auxin homeostasis and metabolism (Fan et al., 2018).

Auxin gradients in plant tissues are established and maintained by the creation of an auxin reflux loop that is largely dependent on PIN-mediated auxin transport (Petrásek and Friml, 2009). The reduced PIN1-GFP and PIN2-GFP abundance at the plasma membrane in *nhx5 nhx6* root tip cells would limit the effective auxin efflux capacity in the root tip. This data is consistent with the slowed root bending and reduced auxin redistribution during root gravitropism in *nhx5 nhx6*, processes which are dependent on PIN2 activity (Abas et al., 2006; Kleine-Vehn et al., 2008). Furthermore, in *nhx5 nhx6* LRP, the limited and diffuse localisation of PIN1-GFP would be sufficient to inhibit cell division and expansion, consistent with our reported defects in lateral root development and emergence. This data is also supported by evidence from single and multiple *pin* mutants which display similar defects in primordia patterning and development (Benková et al., 2003). Likewise, the low penetrance and type of cell patterning defects in *nhx5 nhx6* embryos are strikingly similar to the phenotype of single *pin1* and *pin4* mutant embryos which have reduced auxin transport (Friml et al., 2002; Robert et al., 2015). Thus, our data sugests NHX5 and NHX6 affect auxin gradient establishment through maintaining PIN homeostasis.

NHX5 and NHX6 affect PIN homeostasis independently of polar PIN transport

Published microarray analysis of gene expression in *nhx5 nhx6* whole seedlings revealed no large changes to expression levels in any *PIN* genes (Bassil et al., 2011), suggesting a post-translational mechanism behind the reduction to steady state PIN levels at the plasma membrane. Instead, the sub-cellular trafficking or recycling of PINs to or from the plasma membrane may be altered in *nhx5 nhx6* cells. PINs are constitutively endocytosed to the TGN/EE, and are subsequently recycled back to the plasma membrane through polar transport pathways (Dhonukshe et al., 2007; Friml, 2010; Geldner et al., 2001). BFA washout experiments indicate that the polar delivery and recycling of PIN1 and PIN2 to the plasma membrane is unaffected in *nhx5 nhx6*, also consistent with the lack of defects to PIN1 and PIN2 polarity at the plasma membrane. Furthermore, the non-polar delivery of AUX1 to the plasma membrane occurred normally, suggesting that the general recycling of auxin carriers to the plasma membrane is functional in *nhx5 nhx6*. Thus, NHX5 and NHX6 appear to impact PIN homeostasis

through a pathway independent of polar PIN recycling.

NHX5 and NHX6 may assist in retromer mediated PIN retrieval

While NHX5 and NHX6 are reported to function in vacuolar trafficking of soluble cargo proteins (Ashnest et al., 2015; Bassil et al., 2011; Reguera et al., 2015), their role in the vacuolar trafficking of membrane bound receptors has not been investigated. PIN proteins targeted for degradation are transported to the vacuole via late endocytic pathways, and can be retrieved before degradation from this pathway through retromer complex mediated targeting (Kleine-Vehn et al., 2008; Nodzynski et al., 2013). Thus, retromer activity maintains PIN levels at the TGN/EE for subsequent recycling back to the plasma membrane, assisting in the fine-tuning of PIN abundance at the plasma membrane. We hypothesised that the reduced PIN abundance in *nhx5 nhx6* may be due to a disruption to PIN vacuolar trafficking pathways.

Interestingly, NHX5 and NHX6 mutants share striking phenotypic similarities with retromer mutants. We previously reported that a key component of the retromer complex, SNX1, interacts with the cytosolic tail of NHX6, and colocalises with NHX5 in endosomal compartments (Ashnest et al., 2015). Furthermore, retromer, as well as other mutants associated with defects in protein trafficking to the lytic and protein storage vacuole exhibit sucrose-conditional developmental arrest (Feraru et al., 2010; Kleine-Vehn et al., 2008; Shimada et al., 2006; Silady et al., 2008; Zwiewka et al., 2011), a phenotype attributed to defects in the late steps of the endocytic pathway. Moreover, retromer mutants *snx1* and *vps29* display defects in lateral root growth, reduced gravitropic response, and have reduced PIN1/PIN2 abundance but normal polar PIN recycling (Ambrose et al., 2013; Jaillais et al., 2006, 2007; Kleine-Vehn et al., 2008). The SNX1-NHX6 interaction, together with the reduced PIN abundance but functional polar PIN recycling in *nhx5 nhx6* shown here suggest that NHX5 and NHX6 may assist in the retromer mediated retrieval of PINs.

While we propose that NHX5 and NHX6 facilitate PIN homeostasis through retromer, the mechanism of action is unclear. We hypothesise that NHX5 and NHX6 may be involved in PIN trafficking through the maintenance of pH homeostasis in endomembrane compartments. Recent evidence has shown NHX5 and NHX6 antiporter activity regulates pH homeostasis of the Golgi, TGN/EE, and PVC compartments (Reguera et al., 2015). Furthermore, the disruption to endosomal pH in *nhx5 nhx6* leads

to reduced association of a vacuolar sorting receptor with its cargo (Reguera et al., 2015). In analogy to this, endosomal pH defects in *nhx5 nhx6* could potentially compromise retromer-PIN association, and hence limit PIN retrieval from vacuolar targeting for degradation. Furthermore, we speculate that the NHX6-SNX1 interaction could enable local pH adjustment at the site of retromer binding, which may facilitate PIN binding and retrieval. Future investigation of any pH-sensitivity of retromer-mediated PIN retrieval, including structural analysis of this association, may address this hypothesis.

In conclusion, our data provides new insights into the cellular mechanism of how endosomal Na^+/H^+ antiporters regulate plant growth. We show that NHX5 and NHX6 function during embryo and root development and are required for functional lateral root primordia development and emergence. Moreover, NHX5 and NHX6 mediate auxin gradients and maxima through the maintenance of steady state PIN levels at the plasma membrane. We hypothesise that NHX5 and NHX6 influence PIN protein abundance through late endocytic trafficking pathways, likely involving retromer mediated PIN retrieval.

Materials and Methods

Plant material and growth conditions

Arabidopsis thaliana lines were all in the Columbia-0 (Col-0) accession background. Plant lines used have been previously described: *nhx5-2 nhx6-3* (Ashnest et al., 2015); *pDR5rev::GFP* and *pPIN1::PIN1-GFP* (Benková et al., 2003); *pAUX1::AUX1-YFP* (Swarup et al., 2004); *pPIN2::PIN2-GFP* in *eir1-4* (Xu and Scheres, 2005); and *pNHX6::GUS* (Ashnest et al., 2015).

Seeds were surface sterilized with 70% ethanol for 5 minutes, 10% bleach for 5 minutes, and washed three times in ddH_2O and grown on half-strength Murashige and Skoog (½ MS) medium containing 1.0% (w/v) agar, pH 5.8, without sucrose unless indicated. Seedlings were stratified for 48 hours at 4°C in the dark, and grown in a 16hr light / 8hr dark photoperiod at 22°C.

Wild type (Col-0) lines containing the *pDR5rev::GFP*, *pAUX1-AUX1-YFP*, *pPIN1-PIN1-GFP*, *pPIN2-PIN2-GFP* transgenes were crossed with NHX5/*nhx5-2 nhx6-3*/*nhx6-3* lines. F_1 plants from these initial crosses were selfed and homozygous *nhx5-2 nhx6-3* lines were identified in the segregating F_2 population by PCR genotyping as previously described (Ashnest et al., 2015). Only lines homozygous for the appropriate reporter constructs were used for analysis.

pNHX6:GUS reporter assays

Whole roots from 10 day old Arabidopsis seedlings carrying a 3kb promoter fragment immediately upstream of the start codon of *NHX6* (Ashnest et al., 2015) were fixed in cold 90% acetone for 30 minutes, then washed twice in 100 mM sodium phosphate buffer (pH 7.2) before staining in GUS solution (100 mM sodium phosphate (pH 7.2), 1 mM EDTA, 5 mM potassium ferricyanide, 5 mM potassium ferrocyanide, 1% Triton-X-100 and 1 mg/mL X-Gluc) for 24 hours. Stained tissue was cleared by mounting in Hoyer's solution (70% chloral hydrate, 4% glycerol, 5% gum arabic) and incubating overnight before imaging using a Zeiss Axio Observer inverted microscope.

Microscopy and image quantification

Confocal microscopy was performed using a Zeiss LSM 510 or LSM 780 confocal laser scanning microscope (Carl Zeiss, Germany) with a C-Apochromat 40x/1.2 W or C-Apochromat 40x/1.3 W objective. Excitation and emission detection settings were as follows: GFP/YFP, 488 nm / 490-560 nm, FM5-95, 561 nm / 565-650 nm. For all quantification experiments, identical acquisition settings were used to acquire each image.

Chemical stock solutions were made in DMSO at the following concentrations - BFA 50 mM, CHX 50 mM, FM5-95 (FM4-64 analogue) 4mM, 1-NAA (1-Naphthaleneacetic acid) 10 mM. For BFA treatments, 7-day old seedlings were incubated in 6 well plates containing ½ MS with 50 µM CHX for 60 minutes, 50 µM BFA + 50 µM CHX for 60 minutes, and washed out in in 50 µM CHX for the times indicated. For FM5-95 counter-staining, roots were incubated for 5 minutes at room temperature in ½ MS media containing 2 µM FM5-95 dye, and washed twice in ½ MS before imaging.

For the 1-NAA root elongation experiment, seedlings were grown on ½ MS vertical plates containing 1-NAA at the indicated concentration for 8 days before imaging and analysis. The root length of untreated plants was set at 100%. For the 1-NAA LRP induction experiment, seedlings were first grown on solid ½ MS plates for 4 days and then transferred to solid ½ MS containing 10 µM 1-NAA for 3 days before being imaged by confocal microscopy.

Lateral root phenotyping experiments were performed using seedlings expressing the AUX1:YFP marker grown on ½ MS vertical plates for 15 days. For the *nhx5 nhx6* mutants, only seedlings which

did not arrest growth were used for analysis. For each seedling, the medial slice of each observable lateral root primordia was imaged using a Zeiss Imager M2 fluorescence microscope with a 525/50 nm GFP filter. Primordia were staged similarly to previously described (Lucas et al., 2013; Malamy and Benfey, 1997).

For the root gravitropism experiments, 7-day old seedlings were grown on ½ MS vertical plates before being rotated 90° for the indicated time. The angle of root curvature in at least 30 seedlings per genotype was measured in ImageJ. The *pDR5:GFP* images were by captured by acquiring Z-stacks of 6-8 slices at 2.5 μm per slice, from at least 12 seedlings for each genotype.

Quantification of PIN1-GFP and PIN2-GFP fluorescence was obtained from 15-20 z-stack slices taken at 1 μm intervals, from which a maximum intensity projection was generated. Mean grey values were obtained from the PIN1-GFP or PIN2-GFP localisation region, and subtracted from the mean grey value obtained from the background. Relative fluorescence was calculated with the mean wild type grey value set as 100%.

Post-processing of images was performed with Zeiss ZEN Black (v8.0) and ImageJ v1.48g. Statistical analysis was performed using Microsoft Excel.

Inducible promoter

The NHX6 β-estradiol-inducible rescue construct was generated by ligating the NHX6 ORF into the pMDC7 β-estradiol inducible construct (Curtis and Grossniklaus, 2003). Primer sequences are listed in supplementary material Table S1. To induce NHX6 expression, transgenic *nhx5 nhx6* seed harbouring the inducible NHX6 rescue construct were germinated directly on ½ MS media supplemented with 8 μM β-estradiol (Sigma-Aldrich, E8875). Root lengths and emerged lateral roots were quantified after 14 days. Control media was supplemented with equivalent concentrations of DMSO.

Embryo dissection and analysis

Embryos were dissected from siliques of different developmental stages using hypodermic needles. Embryos were cleared on microscope slides in clearing solution (chloral hydrate: water: glycerol (7:3:1) v/v) and incubated at 4°C for 1 hr. Images were obtained with a Zeiss Axio Observer microscope using 20x air and 63x oil objectives. Embryos were scored by stage from late globular to mid heart according

to ten Hove et al., (2015) in three biological repeats. Embryos were scored as defective if they displayed clear cellular patterning defects in the incipient cotyledon or root cells. For *DR5:GFP* localisation, embryos were dissected from siliques onto microscope slides containing ½ MS liquid and imaged immediately on a LSM 780 confocal laser scanning microscope with a C-Apochromat 40x/1.3 W objective. Only clearly intact embryos were used for analysis.

Funding

This work was supported by an Australian Postgraduate Award to J.D, Graduate Research Scholarships from the Grains Research and Development Corporation to J.A. (GRS 179) and B.F. (GRS 161), by the Government of India, Ministry of Social Justice and Empowerment, National Overseas Scholarship and a La Trobe University Post-Graduate Research Scholarship to P.D., and by an Australian Research Council Linkage Infrastructure, Equipment and Facilities grant (LE0989920).

Disclosures

Conflicts of interest: No conflicts of interest declared.

Acknowledgements

The authors would like to sincerely thank the ABRC, GABI-Kat, D. Smyth, C. Luschnig and T Gaude for supplying seeds, M. Curtis and N.-H. Chua for the pMDC7 vector, the La Trobe Institute for Molecular Science (LIMS) Bioimaging Facility and P. Lock for microscopy assistance, and Ricarda Jost for critical reading of the manuscript.

References

Abas, L., Benjamins, R., Malenica, N., Paciorek, T., Wiśniewska, J., Wirniewska, J., et al., 2006. Intracellular trafficking and proteolysis of the Arabidopsis auxin-efflux facilitator PIN2 are involved in root gravitropism. Nat. Cell Biol. 8, 249–256.

Ambrose, C., Ruan, Y., Gardiner, J., Tamblyn, L.M., Catching, A., Kirik, V., et al., 2013. CLASP interacts with Sorting Nexin 1 to link microtubules and auxin transport via PIN2 recycling in *Arabidopsis thaliana*. Dev. Cell 24, 649–659.

Ashnest, J.R., Huynh, D. Le, Dragwidge, J.M., Ford, B.A., Gendall, A.R., 2015. Arabidopsis intracellular

460 NHX-type sodium-proton antiporters are required for seed storage protein processing. Plant Cell
461 Physiol. 56, 2220–2233.

462 Bassil, E., Coku, A., Blumwald, E., 2012. Cellular ion homeostasis: emerging roles of intracellular NHX
463 Na^+/H^+ antiporters in plant growth and development. J. Exp. Bot. 63, 695–709.

464 Bassil, E., Ohto, M., Esumi, T., Tajima, H., Zhu, Z., Cagnac, O., et al., 2011. The Arabidopsis
465 intracellular Na^+/H^+ antiporters NHX5 and NHX6 are endosome associated and necessary for
466 plant growth and development. Plant Cell 23, 224–239.

467 Benková, E., Michniewicz, M., Sauer, M., Teichmann, T., Seifertová, D., Jürgens, G., et al., 2003. Local,
468 efflux-dependent auxin gradients as a common module for plant organ formation. Cell 115, 591–
469 602.

470 Blilou, I., Xu, J., Wildwater, M., Willemsen, V., Paponov, I., Friml, J., et al., 2005. The PIN auxin efflux
471 facilitator network controls growth and patterning in Arabidopsis roots. Nature 433, 39–44.

472 Blumwald, E., 2000. Sodium transport and salt tolerance in plants. Curr. Opin. Cell Biol. 12, 431–434.

473 Booker, J., Chatfield, S., Leyser, O., 2003. Auxin acts in xylem-associated or medullary cells to mediate
474 apical dominance. Plant Cell 15, 495–507.

475 Bowers, K., Levi, B.P., Patel, F.I., Stevens, T.H., 2000. The sodium/proton exchanger Nhx1p is required
476 for endosomal protein trafficking in the yeast Saccharomyces cerevisiae. Mol. Biol. Cell 11, 4277–
477 4294.

478 Brady, S.M., Orlando, D. a, Lee, J.-Y., Wang, J.Y., Koch, J., Dinneny, J.R., et al., 2007. A high-resolution
479 root spatiotemporal map reveals dominant expression patterns. Science 318, 801–806.

480 Brett, C.L., Donowitz, M., Rao, R., 2005a. Evolutionary origins of eukaryotic sodium/proton exchangers.
481 Am. J. Physiol. Cell Physiol. 288, 223–239.

482 Brett, C.L., Tukaye, D.N., Mukherjee, S., Rao, R., 2005b. The yeast endosomal Na+(K+)/H+ exchanger
483 Nhx1 regulates cellular pH to control vesicle trafficking. Mol. Biol. Cell 16, 1396–1405.

484 Chanroj, S., Wang, G., Venema, K., Zhang, M.W., Delwiche, C.F., Sze, H., 2012. Conserved and

485 diversified gene families of monovalent cation/ H+ antiporters from algae to flowering plants. Front.
486 Plant Sci. 3, 25.

487 Curtis, M.D., Grossniklaus, U., 2003. A gateway cloning vector set for high-throughput functional
488 analysis of genes in planta. Plant Physiol. 133, 462–469.

489 Dhonukshe, P., Aniento, F., Hwang, I., Robinson, D.G., Mravec, J., Stierhof, Y.-D., et al., 2007. Clathrin-
490 mediated constitutive endocytosis of PIN auxin efflux carriers in Arabidopsis. Curr. Biol. 17, 520–
491 527.

492 Dubrovsky, J.G., Sauer, M., Napsucialy-Mendivil, S., Ivanchenko, M.G., Friml, J., Shishkova, S., et al.,
493 2008. Auxin acts as a local morphogenetic trigger to specify lateral root founder cells. Proc. Natl.
494 Acad. Sci. U. S. A. 105, 8790–8794.

495 Fan, L., Zhao, L., Hu, W., Li, W., Novák, O., Strnad, M., et al., 2018. NHX antiporters regulate the pH
496 of endoplasmic reticulum and auxin-mediated development. Plant. Cell Environ.

497 Feraru, E., Paciorek, T., Feraru, M.I., Zwiewka, M., De Groodt, R., De Rycke, R., et al., 2010. The AP-
498 3 β adaptin mediates the biogenesis and function of lytic vacuoles in Arabidopsis. Plant Cell 22,
499 2812–2824.

500 Ford, B.A., Ernest, J.R., Gendall, A.R., 2012. Identification and characterization of orthologs of AtNHX5
501 and AtNHX6 in Brassica napus. Front. Plant Sci. 3, 208.

502 Friml, J., 2010. Subcellular trafficking of PIN auxin efflux carriers in auxin transport. Eur. J. Cell Biol. 89,
503 231–235.

504 Friml, J., Benková, E., Blilou, I., Wisniewska, J., Hamann, T., Ljung, K., et al., 2002. AtPIN4 mediates
505 sink-driven auxin gradients and root patterning in Arabidopsis. Cell 108, 661–673.

506 Geldner, N., Anders, N., Wolters, H., Keicher, J., Kornberger, W., Muller, P., et al., 2003. The
507 Arabidopsis GNOM ARF-GEF mediates endosomal recycling, auxin transport, and auxin-
508 dependent plant growth. Cell 112, 219–230.

509 Geldner, N., Friml, J., Stierhof, Y.D., Jürgens, G., Palme, K., 2001. Auxin transport inhibitors block PIN1

cycling and vesicle trafficking. Nature 413, 425–428.

Jaillais, Y., Fobis-Loisy, I., Miège, C., Rollin, C., Gaude, T., 2006. AtSNX1 defines an endosome for auxin-carrier trafficking in Arabidopsis. Nature 443, 106–109.

Jaillais, Y., Santambrogio, M., Rozier, F., Fobis-Loisy, I., Miège, C., Gaude, T., 2007. The retromer protein VPS29 links cell polarity and organ initiation in plants. Cell 130, 1057–1070.

Kleine-Vehn, J., Dhonukshe, P., Swarup, R., Bennett, M., Friml, J., 2006. Subcellular trafficking of the Arabidopsis auxin influx carrier AUX1 uses a novel pathway distinct from PIN1. Plant Cell 18, 3171–3181.

Kleine-Vehn, J., Leitner, J., Zwiewka, M., Sauer, M., Abas, L., Luschnig, C., et al., 2008. Differential degradation of PIN2 auxin efflux carrier by retromer-dependent vacuolar targeting. Proc. Natl. Acad. Sci. U. S. A. 105, 17812–17817.

Lawrence, S.P., Bright, N. a, Luzio, J.P., Bowers, K., 2010. The sodium/proton exchanger NHE8 regulates late endosomal morphology and function. Mol. Biol. Cell 21, 3540–3551.

Lucas, M., Kenobi, K., von Wangenheim, D., Voβ, U., Swarup, K., De Smet, I., et al., 2013. Lateral root morphogenesis is dependent on the mechanical properties of the overlaying tissues. Proc. Natl. Acad. Sci. U. S. A. 110, 5229–5234.

Malamy, J.E., Benfey, P.N., 1997. Organization and cell differentiation in lateral roots of Arabidopsis thaliana. Development 124, 33–44.

Marchant, A., Bhalerao, R., Casimiro, I., Eklöf, J., Casero, P.J., Bennett, M., et al., 2002. AUX1 promotes lateral root formation by facilitating indole-3-acetic acid distribution between sink and source tissues in the Arabidopsis seedling. Plant Cell 14, 589–597.

Möller, B., Weijers, D., 2009. Auxin control of embryo patterning. Cold Spring Harb. Perspect. Biol.

Naramoto, S., Otegui, M.S., Kutsuna, N., De Rycke, R., Dainobu, T., Karampelias, M., et al., 2014. Insights into the localization and function of the membrane trafficking regulator GNOM ARF-GEF at the Golgi apparatus in Arabidopsis. Plant Cell 26, 3062–3076.

Nodzynski, T., Feraru, M.I., Hirsch, S., De Rycke, R., Niculaes, C., Boerjan, W., et al., 2013. Retromer subunits VPS35A and VPS29 mediate prevacuolar compartment (PVC) function in Arabidopsis. Mol. Plant 6, 1849–1862.

Ohgaki, R., Matsushita, M., Kanazawa, H., Ogihara, S., Hoekstra, D., van Ijzendoorn, S.C.D., 2010. The Na^+/H^+ exchanger NHE6 in the endosomal recycling system is involved in the development of apical bile canalicular surface domains in HepG2 cells. Mol. Biol. Cell 21, 1293–1304.

Ohgaki, R., van IJzendoorn, S.C.D., Matsushita, M., Hoekstra, D., Kanazawa, H., 2011. Organellar Na+/H+ exchangers: novel players in organelle pH regulation and their emerging functions. Biochemistry 50, 443–450.

Orlowski, J., Grinstein, S., 2007. Emerging roles of alkali cation/proton exchangers in organellar homeostasis. Curr. Opin. Cell Biol. 19, 483–492.

Petrásek, J., Friml, J., 2009. Auxin transport routes in plant development. Development 136, 2675–2688.

Reguera, M., Bassil, E., Tajima, H., Wimmer, M., Chanoca, A., Otegui, M.S., et al., 2015. pH regulation by NHX-type antiporters is required for receptor-mediated protein trafficking to the vacuole in Arabidopsis. Plant Cell 27, 1200–1217.

Robert, H.S., Grunewald, W., Sauer, M., Cannoot, B., Soriano, M., Swarup, R., et al., 2015. Plant embryogenesis requires AUX/LAX-mediated auxin influx. Development 142, 702–711.

Robert, S., Chary, S.N., Drakakaki, G., Li, S., Yang, Z., Raikhel, N. V, et al., 2008. Endosidin1 defines a compartment involved in endocytosis of the brassinosteroid receptor BRI1 and the auxin transporters PIN2 and AUX1. Proc. Natl. Acad. Sci. U. S. A. 105, 8464–8469.

Scarpella, E., Marcos, D., Friml, J., Berleth, T., 2006. Control of leaf vascular patterning by polar auxin transport. Genes Dev. 20, 1015–1027.

Shimada, T., Koumoto, Y., Li, L., Yamazaki, M., Kondo, M., Nishimura, M., et al., 2006. AtVPS29, a putative component of a retromer complex, is required for the efficient sorting of seed storage proteins. Plant Cell Physiol. 47, 1187–1194.

561 Silady, R.A., Ehrhardt, D.W., Jackson, K., Faulkner, C., Oparka, K., Somerville, C.R., 2008. The
562 GRV2/RME-8 protein of Arabidopsis functions in the late endocytic pathway and is required for
563 vacuolar membrane flow. Plant J. 53, 29–41.

564 Spitzer, C., Reyes, F.C., Buono, R., Sliwinski, M.K., Haas, T.J., Otegui, M.S., 2009. The ESCRT-related
565 CHMP1A and B proteins mediate multivesicular body sorting of auxin carriers in Arabidopsis and
566 are required for plant development. Plant Cell 21, 749–766.

567 Swarup, R., Kargul, J., Marchant, A., 2004. Structure-function analysis of the presumptive Arabidopsis
568 auxin permease AUX1. Plant Cell 16, 3069–3083.

569 Swarup, R., Swarup, R., Marchant, A., Marchant, A., Ljung, K., Ljung, K., et al., 2001. Localization of
570 the auxin permease AUX1 suggests two functionally distinct hormone transport pathways operate
571 in the Arabidopsis root apex. Genes Dev. 15, 2648–2653.

572 ten Hove, C.A., Lu, K.-J., Weijers, D., 2015. Building a plant: cell fate specification in the early
573 Arabidopsis embryo. Development 142, 420–430.

574 Vilches-Barro, A., Maizel, A., 2015. Talking through walls: mechanisms of lateral root emergence in
575 *Arabidopsis thaliana*. Curr. Opin. Plant Biol. 23, 31–38.

576 Viotti, C., Bubeck, J., Stierhof, Y.-D., Krebs, M., Langhans, M., van den Berg, W., et al., 2010. Endocytic
577 and secretory traffic in Arabidopsis merge in the trans-Golgi network/early endosome, an
578 independent and highly dynamic organelle. Plant Cell 22, 1344–1357.

579 Wisniewska, J., Xu, J., Seifertová, D., Brewer, P.B., Ružička, K., Blilou, I., et al., 2006. Polar PIN
580 localization directs auxin flow in plants. Science 312, 883–883.

581 Xu, J., Scheres, B., 2005. Dissection of Arabidopsis ADP-RIBOSYLATION FACTOR 1 function in
582 epidermal cell polarity. Plant Cell 17, 525–536.

583 Yokoi, S., Quintero, F.J., Cubero, B., Ruiz, M.T., Bressan, R.A., Hasegawa, P.M., et al., 2002.
584 Differential expression and function of Arabidopsis thaliana NHX Na+/H+ antiporters in the salt
585 stress response. Plant J. 30, 529–539.

586 Zwiewka, M., Feraru, E., Möller, B., Hwang, I., Feraru, M.I., Kleine-vehn, J., et al., 2011. The AP-3
587 adaptor complex is required for vacuolar function in Arabidopsis. Cell Res. 21, 1711–1722.

588

Legends to figures

Figure 1: Lateral root development and emergence are inhibited in *nhx5 nhx6*.

(A) *pNHX6::GUS* expression pattern in the primary root tip and lateral root primordia (stages denoted by roman numerals; Em, emerged; LR, lateral root).

(B) Confocal images of lateral root primordia expressing AUX1-YFP through early and late developmental stages.

(C-E) Quantification of mean root length (C), lateral root primordia density (D), and distribution of lateral root primordia (E) from the primary root of 15 day old seedlings expressing AUX1-YFP. For each seedling, developing lateral root primordia along the primary root were staged as per Malamy and Benfey (1997), and the proportion of each stage was quantified from the total amount of initiated primordia. Data are means ± s.e.m. of >15 seedlings. Students t-test; *$p < 0.05$; **$p < 0.01$. Scale bars = 20 μm.

Figure 2. NHX5 and NHX6 are involved in auxin-mediated embryo development.

Morphology of cleared embryos from globular to heart stage. Arrows and indicate the position and region of aberrant cell division and patterning in *nhx5 nhx6* embryos compared to wild type. Brackets indicate the basal embryo domain where cell division defects were most prevalent. The number of embryos examined and the penetrance of embryos displaying defects in morphology is indicated. Scale bars = 10 μm.

Figure 3. Auxin gradients are disrupted in *nhx5 nhx6*.

(A) *DR5::GFP* expression in the primary root tip of 7 day old seedlings. Counterstain in red is FM5-95.

(B) *DR5::GFP* expression in late stage lateral root primordia. Note the diffuse expression and reduced DR5 auxin maxima in the tips of *nhx5 nhx6* compared to wild type (arrowheads).

(C) *DR5::GFP* expression in triangle and heart stage embryos. Reduced DR5 expression is present in meristem derived tissue (arrows), and in the apical tips (arrowheads) in *nhx5 nhx6* compared to wild type. Penetrance of auxin signaling defects in heart stage embryos are indicated. Scale bars = 20 μm.

Figure 4. Auxin perception and gravitropism response is altered in *nhx5 nhx6*.

(A) Relative root elongation of seedlings grown on medium supplemented with 1-NAA. Data are means

± s.e.m. of > 20 seedlings. Students t-test; **p < 0.01.

(B) Lateral root initiation in *DR5::GFP* seedlings after treatment with 10 µM 1-NAA for 72 hrs. Note the reduction of late stage developed LRP (arrows) and presence of underdeveloped LRP (arrowheads) in *nhx5 nhx6*.

(C) Quantification of LRP development from (B). LRP were scored as developing (Stage I to Stage VII) or emerged. At least 8 roots were examined for each genotype.

(D) Time course of root curvature after gravity stimulus. Data are means ± s.e.m. of >30 seedlings. Students t-test; *p < 0.05; **p < 0.01.

(E) Auxin distribution in response to gravity stimulus visualised by *DR5::GFP* 2 hr after reorientation. Scale bars = 50 µm (A), 20 µm (E).

Figure 5. PIN1 and PIN2 abundance are reduced in *nhx5 nhx6.*

(A-C) Maximum intensity projections of AUX1-YFP (A), PIN1-GFP (B), and PIN2-GFP (C), in the primary root tip of 7 day old seedlings.

(D) Quantification of relative AUX1-YFP, PIN1-GFP and PIN2-GFP fluorescence. Data represents the means ± s.e.m from n ≥ 9 seedlings. Students t-test; * p < 0.05, ** p < 0.01.

(E) Localisation of PIN1-GFP in developing lateral root primordia. Note the reduction in PIN1-GFP levels in *nhx5 nhx6* LRP during stage V to VII. Scale bars = 20 µm.

Figure 6. NHX5 and NHX6 are not directly required for polar PIN1 and PIN2 recycling.

BFA washout experiment. Root epidermal cells expressing PIN1-GFP and PIN2-GFP were pre-treated with Cycloheximide (CHX) for 1hr to inhibit protein synthesis, then incubated with Brefeldin A (BFA) + CHX for 1 hr, before being washed in CHX for the indicates times. Note the presence of BFA bodies (arrowheads) after BFA treatment, and absence of BFA bodies after washout in both wild type and *nhx5 nhx6* cells.

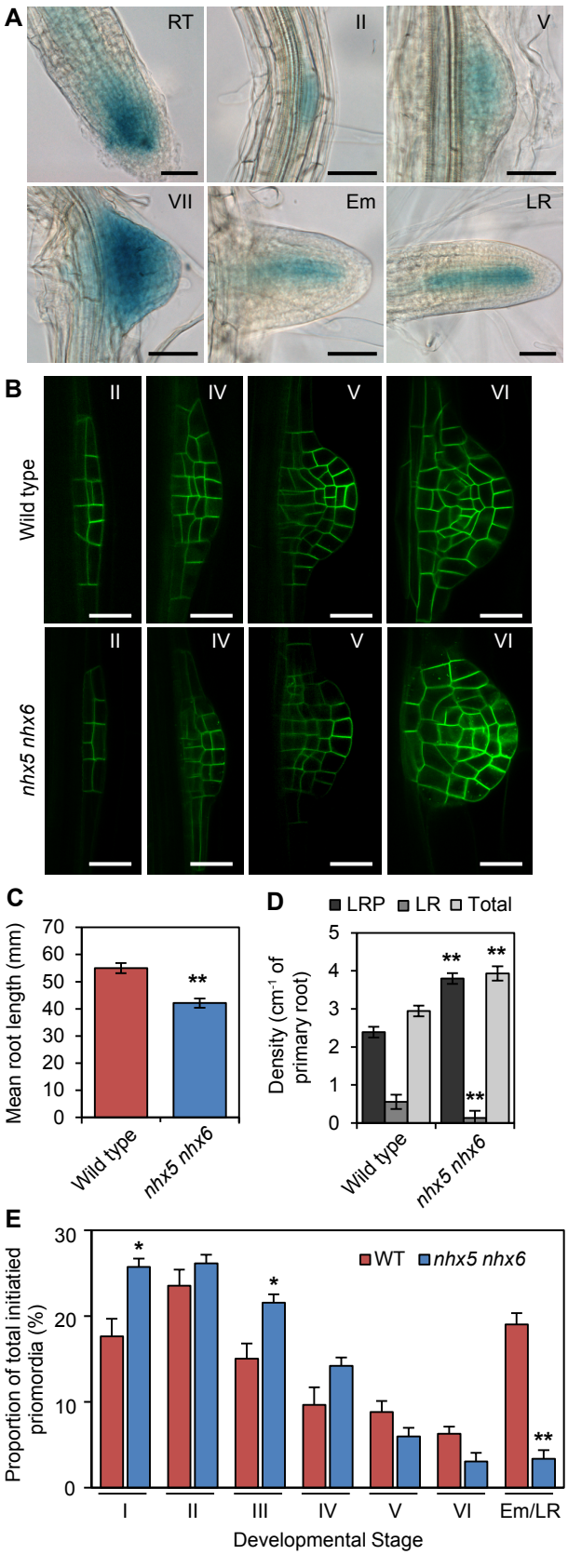
A
RT
II
V
VII
Em
LR
B
Wild type
nhx5 nhx6
II
IV
V
VI
C
Mean root length (mm)
70
60
50
40
30
20
10
0
**
Wild type
nhx5 nhx6
D
LRP
LR
Total
Density (cm-1 of primary root)
5
4
3
2
1
0
**
**
**
Wild type
nhx5 nhx6
E
Proportion of total initiatied priomordia (%)
30
20
10
0
*
*
**
WT
nhx5 nhx6
I
II
III
IV
V
VI
Em/LR
Developmental Stage

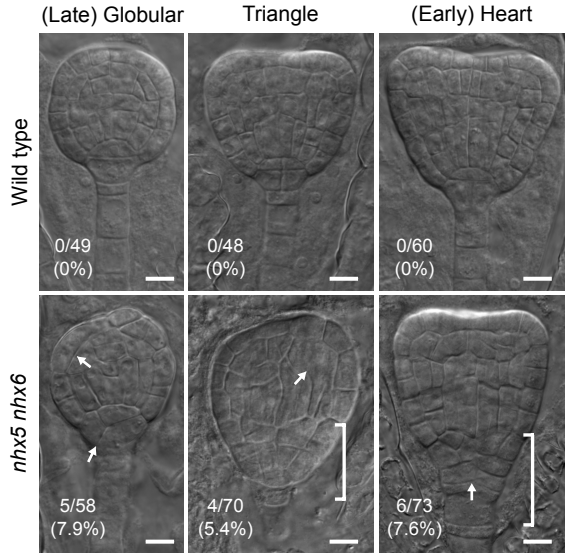
(Late) Globular
Triangle
(Early) Heart
Wild type
nhx5 nhx6
0/49
(0%)
0/48
(0%)
0/60
(0%)
5/58
(7.9%)
4/70
(5.4%)
6/73
(7.6%)

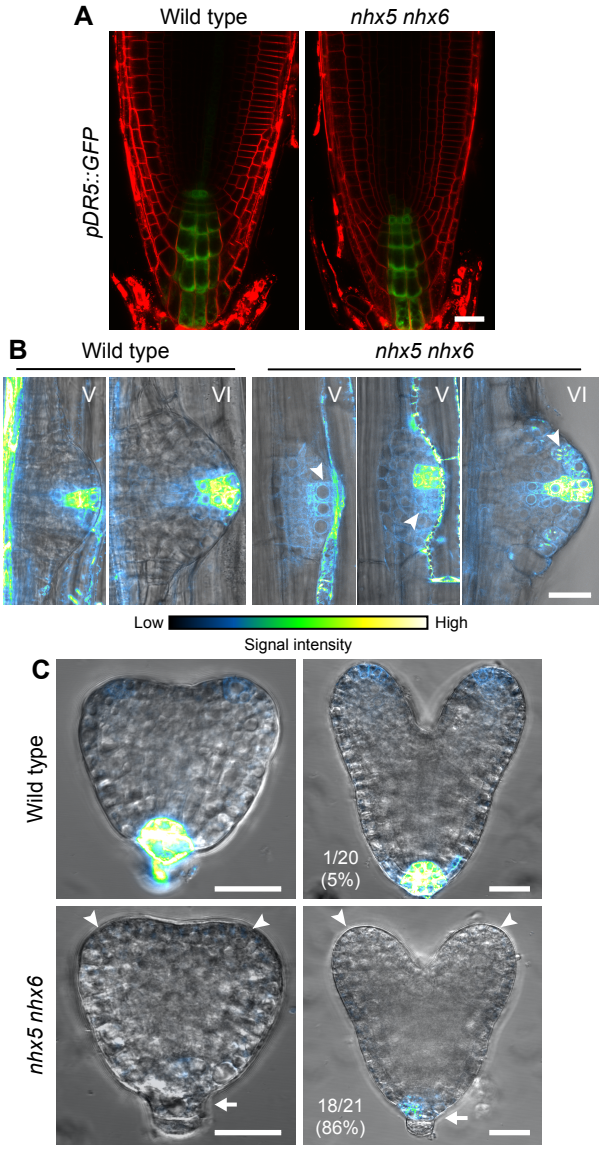
A
Wild type
nhx5 nhx6
pDR5::GFP
B
Wild type
nhx5 nhx6
V
VI
V
V
VI
Low
High
Signal intensity
C
Wild type
nhx5 nhx6
1/20
(5%)
18/21
(86%)

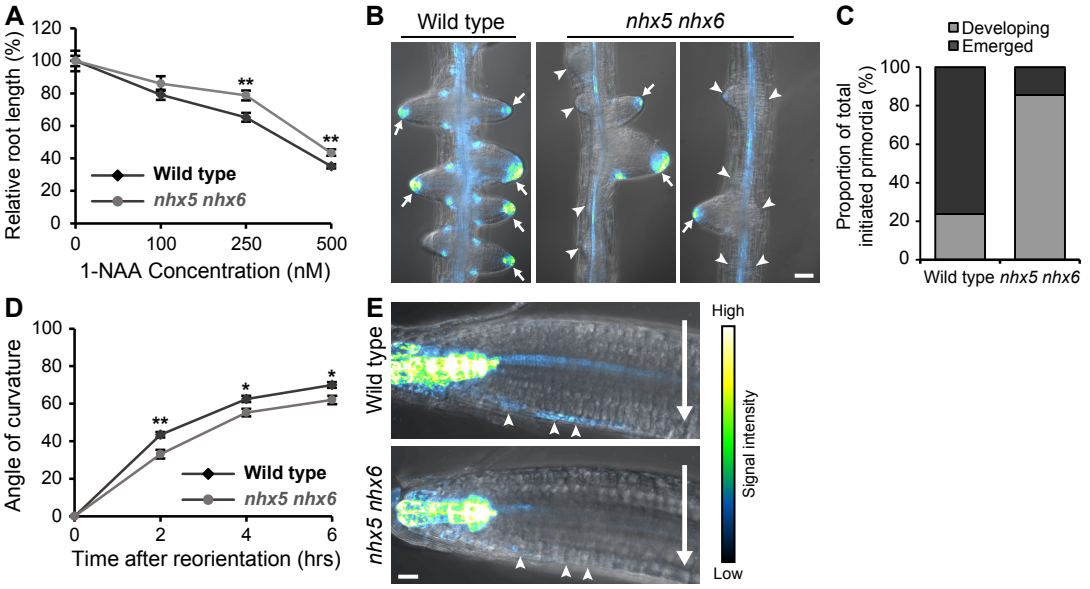
A
Relative root length (%)
120
100
80
60
40
20
0
0
100
250
500
1-NAA Concentration (nM)
**
**
Wild type
nhx5 nhx6
B
Wild type
nhx5 nhx6
C
Developing
Emerged
Proportion of total initiated primordia (%)
100
80
60
40
20
0
Wild type
nhx5 nhx6
D
Angle of curvature
100
80
60
40
20
0
0
2
4
6
Time after reorientation (hrs)
**
*
*
Wild type
nhx5 nhx6
E
Wild type
nhx5 nhx6
High
Signal intensity
Low

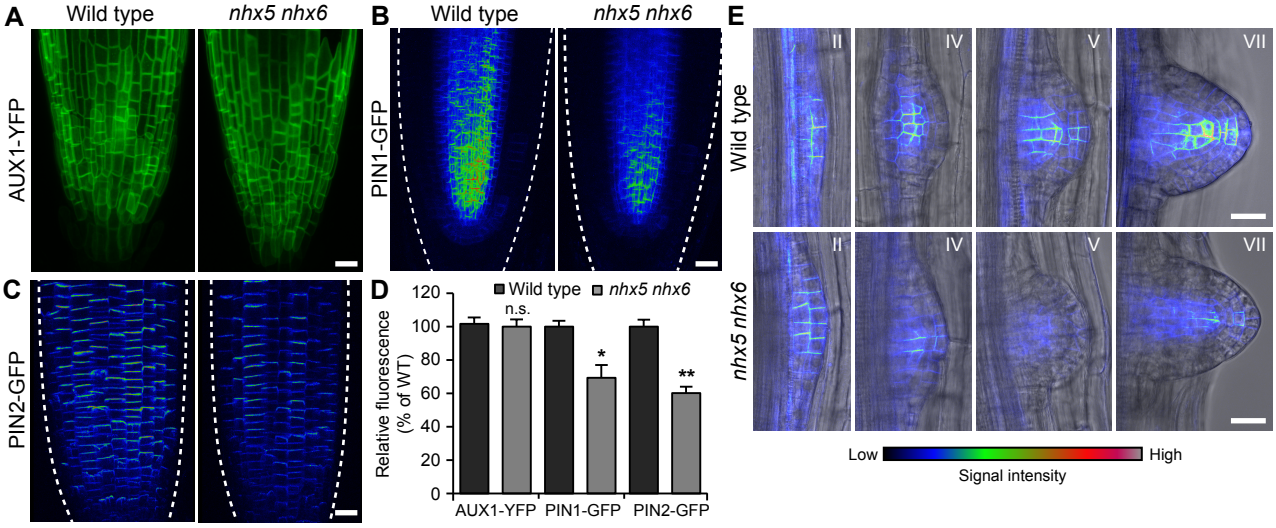
A
Wild type
nhx5 nhx6
AUX1-YFP
B
Wild type
nhx5 nhx6
PIN1-GFP
C
PIN2-GFP
D
Wild type
nhx5 nhx6
Relative fluorescence (% of WT)
120
100
80
60
40
20
0
n.s.
*
**
AUX1-YFP
PIN1-GFP
PIN2-GFP
E
Wild type
nhx5 nhx6
II
IV
V
VII
Low
High
Signal intensity

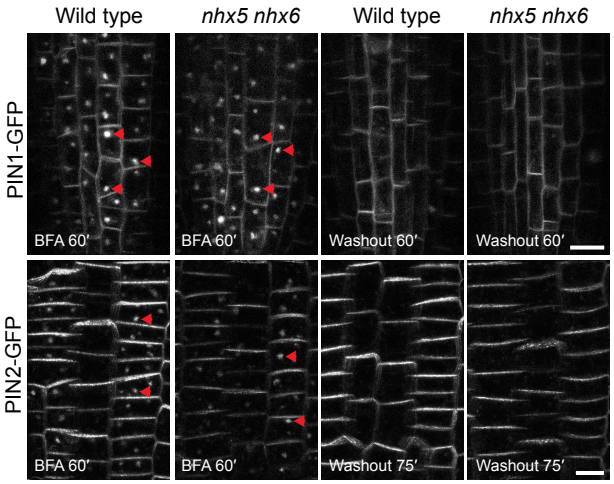
Wild type
nhx5 nhx6
Wild type
nhx5 nhx6
PIN1-GFP
PIN2-GFP
BFA 60′
BFA 60′
Washout 60′
Washout 60′
BFA 60′
BFA 60′
Washout 75′
Washout 75′